

How do Materials Fracture? - In Situ and Non-Destructive Observation of Crack Initiation and Propagation in Carbon-Fiber Reinforced Plastic (CFRP) -

The nanoscopic mechanism of crack initiation and propagation in carbon-fiber reinforced plastic (CFRP) was revealed by *in situ* and nondestructive observation using synchrotron-radiation X-ray Computed Tomography (X-CT). It was found that voids and cracks do not simply result from local stresses but instead occur largely via two competing nanoscale mechanisms, namely, *fiber/plastic interface debonding* and *in-plastic crack initiation*. Therefore, nanoscopic insights into these heterogeneities are essential for controlling crack initiation and determining reasonable safety margins for the use of CFRP composite.

Although voids and cracks can fatally degrade structural materials such as metals and ceramics, they are tolerated in carbon fiber-reinforced plastic (CFRP) composites if monitored to ensure their growth remains below a critical size. Thus, the use of CFRPs as aeronautical structural materials requires an understanding of multi-scale crack formation (Fig. 1). However, the mechanism of crack formation at the nanoscopic scale remains unclear because experimental difficulties have hindered studies of relevant phenomena occurring *prior* to crack formation. In this report, we detail high-resolution (~50 nm) and nondestructive three-dimensional observations of crack initiation and propagation under applied stress [1, 2].

First, we examined cracking by *in situ* observations made via macroscopic X-CT. The macroscopic X-CT results showed that transverse cracks (a few hundred micrometers) first appeared in the 90° plies (=sheets) at ~40–50% of the fracture strength (σ_f), and their propagation accelerated two-folds with an 10% increase in tensile stress.

Then, we utilized a technique developed specifically to observe crack initiation, nanoscopic X-CT using synchrotron radiation (SR X-CT), that couples phase-contrast X-CT and transmission X-ray microscopy using synchrotron radiation to achieve a spatial resolution of ~50 nm. The relatively small density difference between carbon fibers and the plastic matrix in CFRPs makes it challenging to obtain high-contrast images at a smaller scale (sub-micrometer) using conventional absorption-contrast X-CT measurements.

A columnar specimen with unidirectional carbon fibers was mechanically loaded with a diamond indenter using a nanomechanical test stage, which simulates crack initiation in the 90° plies (Fig. 1). *In situ* observations under stress were performed using the nanoscopic SR X-CT. First, the diamond indenter was inserted to initiate small pre-cracks. Subsequently, the extent of insertion was increased with a step from 0.1 to 1.0 μm , resulting in the propagation of a single crack. Finally, we focused on the region around the crack tip and repeated the CT measurement cycle.

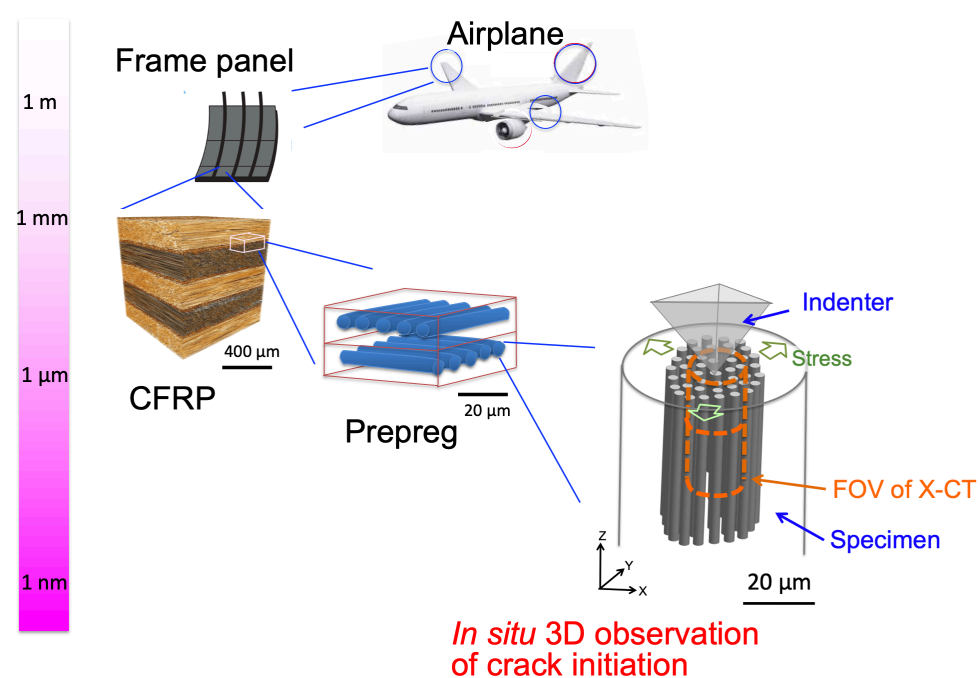


Figure 1: Multi-scale observation of CFRP [1].

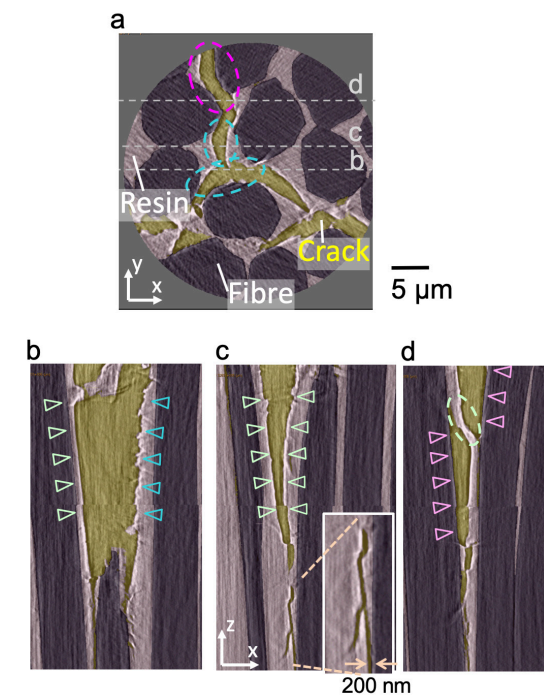


Figure 2: Segmented images of cracks formed in the CFRP. **a**, X-Y, and **b, c, d**, X-Z cross-sectional images corresponding to sections along broken lines **b, c**, and **d** in **a**. Carbon fibers, plastic resin, and cracks (air) are shown in purple, grey, and yellow, respectively. **b, c** typical *in-plastic crack initiation* with smooth (green triangles) and rough (blue triangles) crack surfaces. **d** *fiber/plastic interface debonding* (red triangles). Branching at the crack tip (inset in **c**) and plastic bridges between interfaces (broken line in **d**) are also clearly observed. [1].

Figure 2 shows typical examples of cross-sectional images based on reconstructed 3D volume data and segmentation results. In the case of conventional absorption-contrast imaging, the segmentation can be easily performed by determining threshold values based on the contrast (i.e., absorption) of the reconstructed 3D volume data because each component of the material has a different contrast value. However, in the case of phase-contrast imaging, segmentation is much more challenging because the various components of the material have similar contrast values, and the contrast difference is emphasized only at the component boundaries (black–white fringes). Therefore, we segmented the 3D volume images using the Fiji image processing software’s “watershed segmentation” feature of the “Morphological segmentation” plugin for the cracks, and a deep learning approach using SegNet and MATLAB for the carbon fibers [1].

At the nanoscale, the initiation of cracks was location-dependent and heterogeneous, and two competing processes, *fiber/plastic interface debonding* and *in-plastic crack initiation*, were observed. In the former process, *fiber/plastic interface debonding*, cracks were initiated by opening the fiber/plastic interfaces measuring ~100–200 nm and propagated along the fiber/plastic boundary (Fig. 2d).

In the latter process, small voids (Fig. 2a, b) were initiated and propagated via plastic deformation. These cracks traveled across the plastic matrix to neighboring fibers, propagated within the plastic in the Z-direction

along a path with rough or smooth crack surfaces, or branching into two or more cracks.

Local stress was shown to be largely dependent on location at the nanoscopic scale. Moreover, the thickness of the epoxy resin plays an important role due to its effects on the alignment of the carbon fibers. Depending on the resin thickness, deviation from the ideal alignment of the carbon fibers may occur [2]. Variation in epoxy thickness is inevitable during industrial processing of CFRP, and the information on its effects on cracking is of great importance.

Our evaluation reveals that voids and cracks do not simply result from local stresses, but instead occur largely via two specific competing nanoscale mechanisms: *fiber/plastic interface debonding* and *in-plastic crack initiation*. Further insight into these heterogeneities at the nanoscopic level is essential for controlling crack initiation and determining reasonable safety margins for CFRP composite use.

REFERENCES

- [1] M. Kimura, T. Watanabe, Y. Takeichi and Y. Niwa, *Sci. Rep.* **9**, 19300 (2019).
- [2] T. Watanabe, Y. Takeichi, Y. Niwa, M. Hojo and M. Kimura, *Compos. Sci. Technol.* **197**, 108244 (2020).

BEAMLINE

AR-NW2A

M. Kimura^{1,2}, T. Watanabe¹, Y. Takeichi^{1,2}, Y. Niwa¹ (KEK-IMSS-PF, ²SOKENDAI)